J. Biochem. **141**, 121–126 (2007)
doi:10.1093/jb/mvm015

Process of Maturation of Tetraheme Cytochrome c_3 in a *Shewanella* Expression System

Yuki Takayama[1,2], Yehua Shen[1,†] and Hideo Akutsu[1,*]

[1]Institute for Protein Research, Osaka University, 3-2 Yamadaoka, Suita, Osaka 565-0871, and [2]Institute for Bioinformatics Research and Development, Japan Science and Technology Agency, 5-3 Yonbancho, Chiyoda, Tokyo 102-8666, Japan

Received September 25, 2006; accepted November 23, 2006; published online December 13, 2006

The process of maturation of multiheme proteins is not yet well known, while that of monoheme ones has been relatively well investigated. Two kinds of partly unfolded tetraheme cytochrome c_3 were obtained on overexpression in *Shewanella oneidensis* TSP-C. These proteins were characterized by circular dichroism and nuclear magnetic resonance spectroscopy. It turned out that the tetraheme architecture, and the fifth and sixth ligand coordination are almost mature, while some parts of the polypeptide are unfolded. The unfolded residues are mainly located in the helix-rich region including heme attachment and axial ligand sites. This suggests that the formation of the heme architecture, coordination of axial ligands and helix formation should be coupled with each other. While the former two can take place automatically, the helix formation would need help by a chaperone-like function in the cytochrome *c* maturation (Ccm) machinery. It must be working in sulphate-reducing bacteria. The Ccm machinery in *S. oneidensis* is likely insufficient to help the maturation of proteins with cyclic heme architectures. This is the first report providing an insight into the process of maturation of tetraheme cytochrome c_3.

Key words: chaperon, cytochrome c_3, cytochrome *c* maturation, folding, heme architecture, sulphate-reducing bacterium.

Abbreviations: cyt, cytochrome; SRB, sulphate-reducing bacteria; *D*vMF, *Desulfovibrio vulgaris* Miyazaki F; Ccm, cytochrome *c* maturation; NaP_i, sodium phosphate; CD, circular dichroism; NMR, nuclear magnetic resonance; Gdn-HCl, guanidine hydrochloride.

A *c*-type cytochrome possesses hemes linked covalently to a polypeptide. The heme attachment process on the periplasmic side of the membrane has been extensively studied [reviewed in (*1*)]. The maturation of *c*-type cytochromes needs a series of membrane enzymes, which catalyse the transportation of a cytochrome peptide across the membrane, linking of a protoheme to two Cys residues in the peptide through thioether bonds, coordination of ligands and folding of the peptide. The presence of the fifth His has been indicated to be essential for the heme linking process (*2*). Although the transportation and attachment of the heme have been relatively well characterized, the folding process has not been elucidated yet. In contrast, the folding of monoheme cytochrome *c* (cyt *c*) *in vitro* has been extensively studied [reviewed in (*3*)]. According to these studies, a folding of cyt *c* can be divided into five steps: (i) incorporation of heme into the polypeptide, (ii) coordination of the fifth ligand, (iii) partial formation of secondary structure, (iv) coordination of the sixth ligand and (v) complete formation of the tertiary structure (*3*). However, there have been few reports on the maturation or folding of multiheme cytochromes.

Cyt c_3 isolated from sulphate-reducing bacteria (SRB) is a small soluble protein (typically ca. 14 kDa) and possesses four *c*-type hemes in a single polypeptide. This protein has been classified as a class III *c*-type cytochrome (*4*). It is an electron transport protein and plays an important role in sulphate respiration. The three-dimensional structures of ferric and ferrous forms of cyt c_3 from an SRB, *Desulfovibrio vulgaris* Miyazaki F (*D*vMF) used in this study, have been determined (*5–7*). Since *c*-type heme is covalently linked to a polypeptide, the maturation of cyt c_3 needs special machinery comprising cytochrome *c* maturation (Ccm) proteins as well as cyt *c*. Because of the low efficiency of the machinery, an expression system in *Escherichia coli* can only produce apoproteins under aerobic conditions (*8, 9*). Later, three heterogeneous expression systems that can produce holo-cyt c_3 were reported. Namely, cyt c_3 was expressed in purple photosynthetic bacteria (*10*), in *E. coli* (*11, 12*) with co-expression of the *ccm* genes (*13*), and in *Shewanella oneidensis* TSP-C (*14*). The common feature of these expression systems is that the type I Ccm system works in the host cell as in the case of SRB [reviewed in (*15, 16*)].

Although the type I Ccm system works correctly in the expression of cyt c_3 in *S. oneidensis* (*14*, *17*), a small amount of misfolded proteins was obtained like

†Current address: Department of Chemistry, Northwest University, China.
*To whom correspondence should be addressed. Tel: +81-6-6879-8597. Fax: +81-6-6879-8599.
E-mail: akutsu@protein.osaka-u.ac.jp

in the case of cytochrome b_{562} expressed in *E. coli* (*18*). We have characterized the misfolded cyts c_3 and discussed the folding of tetraheme protein cyt c_3 in the maturation process on the basis of the obtained results.

MATERIALS AND METHODS

Growth and purification—*Dv*MF cyt c_3 was produced in *S. oneidensis* TSP-C transformed with pKFC3 (*19*) harboruing the *Dv*MF cyt c_3 gene, as described previously (*17*). ^{15}N-labelled cyt c_3 was produced using ^{15}N-labelled CHL medium (Chlorella Industry Co., Ltd.), as described previously (*20*). The transformants were microaerobically grown and cyt c_3 was purified as described previously (*21*). The purification process mainly comprises three steps, 70% saturated ammonium sulphate [$(NH_4)_2SO_4$] fractionation, hydrophobic column chromatography and cation-exchange column chromatography at 4°C. Two kinds of misfolded cyts c_3 were obtained during the purification process, namely, misfolded A and B (mfA and mfB) cyts c_3. The intact and mfB cyts c_3 could be purified by the same method. They were eluted with 140 and 300 mM sodium chloride on cation-exchange column chromatography, respectively. MfA cyt c_3, however, was precipitated on 70% saturated $(NH_4)_2SO_4$ fractionation, and did not adsorb to the cation-exchange resin. It was purified at 4°C as follows. The precipitate obtained at 70% $(NH_4)_2SO_4$ saturation was dissolved in a 30 mM sodium phosphate (NaP_i) buffer, pH 7.0, and then $(NH_4)_2SO_4$ was added to the solution, up to 50% saturation, which was centrifuged at 12 000 g for 30 min. The supernatant was passed through a 0.22 μm filter, loaded onto a Phenyl-Sepharose 26/10 column (Amersham Bioscience) equilibrated with 50% saturated $(NH_4)_2SO_4$ in 30 mM NaP_i, pH 7.0, and then eluted with a gradient of 50–0% saturated $(NH_4)_2SO_4$ in 30 mM NaP_i, pH 7.0. The cyt c_3 fractions were collected, dialysed against 30 mM NaP_i, pH 7.0, and then concentrated with a Centricon YM-10 (Millipore) to roughly 2 ml. The sample was loaded onto a Q-Sepharose 16/10 column (Amersham Bioscience) equilibrated with 30 mM NaP_i, pH 7.0. The non-adsorbed fraction was collected, dialysed against ultra-pure water and then lyophilized. The purity was checked by SDS-polyacrylamide gel electrophoresis.

Circular Dichroism Measurements—Circular dichroism (CD) spectra were acquired with a Jasco J-720WI CD spectropolarimeter at 30°C using a 1 mm path length quartz cell. The sample concentrations were 4 μM for the far-UV region (190–250 nm) and 14 μM for the Soret-band (380–440 nm) region in 30 mM NaP_i, pH 7.0, respectively. A solvent spectrum obtained under the same conditions was subtracted from the observed one to obtain the actual sample spectrum. The results are expressed in mean residue ellipticity.

Nuclear Magnetic Resonance Measurements—0.5–1 mM protein was dissolved in 30 mM NaP_i/99.96% ^2H_2O, p^{2}H 7.0. Nuclear magnetic resonance (NMR) spectra at 500 and 600 MHz were recorded at 303 K with Bruker AVANCE DRX-500 and DRX-600 NMR spectrometers (Bruker), respectively. Chemical shifts are presented in parts per million (ppm) relative to 2,2-dimethyl-2-silapentane-5-sulphonate as an internal reference.

Refolding of mfA and mfB cyts c_3—The misfolded A (mfA) and B (mfB) cyts c_3 were dissolved in 6 M guanidine hydrochlororide (Gdn-HCl) or 8 M urea in 30 mM NaP_i, pH 7.0, and then dialysed against 2.5 l of the same buffer at 4°C overnight. The concentration of the denaturant was gradually reduced by dialysis, as follows. 30 mM NaP_i buffer, pH 7.0, was added to the dialysed buffer at 5 ml/min. After the concentration of the denaturant had reached <1 mM, the sample was purified on a cation-exchange column as mentioned above.

RESULTS

There were three forms of *Dv*MF cyt c_3 expressed in *S. oneidensis*. They are designated as mfA, mfB and intact cyts c_3 in this work. The weight ratio of mfA, mfB and intact cyts c_3 was roughly 2:2:9 (Table 1). The temperature dependence of the growth yield was examined in the range of 22–30°C. The lower the temperature was, the higher the yield of cells was. There was an optimal temperature for the production of intact cyt c_3 in the *Shewanella* expression system, i.e. 25°C (Table 1). The fractions of the misfolded proteins, however, depended neither on the rate of growth of cells nor on the rate of production of cyt c_3 (Table 1). N-terminus analysis (15 amino acid residues) and MALDI-TOF (matrix-assisted laser desorption ionization time of flight) mass spectroscopy (Fig. S1 of the supplementary material, available at *JB* online) of the three kinds of cyt c_3 gave the same results, showing the polypeptides and thioether linkages between the polypeptides and hemes were intact even for mfA and mfB cyts c_3. Although there are eight cysteine residues, only intact thioether linkages are possible because heme binding motifs (CXXCH and CXXXXCH, where X is any amino acid residue) can form the linkage only through enzymatic reactions (*1*).

The CD spectra of mfA, mfB and intact cyts c_3 are shown in Fig. 1. Although there were only slight changes in the Soret-band region, the secondary structure content was reduced for mfA and mfB cyts c_3. This indicated that the tetraheme architecture was almost mature, while a part of the secondary structure was lacking in both misfolded proteins, as in the case of the molten globule structure of cytochrome b_{562} (*18*). Here, we define the heme architecture as a macroscopic configuration of four hemes determined by relative orientations of heme rings and inter-heme distances, which would mainly affect the CD in the Soret-band region (*21*). Further characterization was carried out by NMR spectroscopy to examine the details of the effect on the structure.

Table 1. **The temperature dependence of the yields of wet cells (g/l culture) and the three kinds of cytochrome c_3 (mg/l culture) expressed in *S. oneidensis* TSP-C.**

Temperature	Wet cells	MfA cyt c_3	MfB cyt c_3	Intact cyt c_3
22°C	6.89	1.66	1.68	6.82
25°C	6.20	2.06	2.09	9.61
27°C	4.52	1.69	1.72	7.96
30°C	3.27	1.70	1.71	7.10

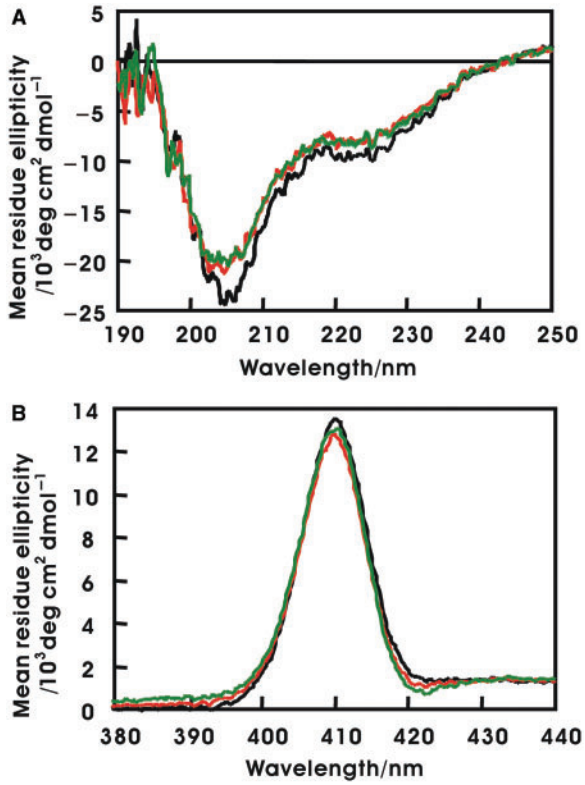

Fig. 1. **Circular dichroism spectra of misfolded A (red), B (green) and intact (black) cytochromes c_3 at pH 7.0 and 30°C**. (A) Far-UV and (B) Soret-band regions.

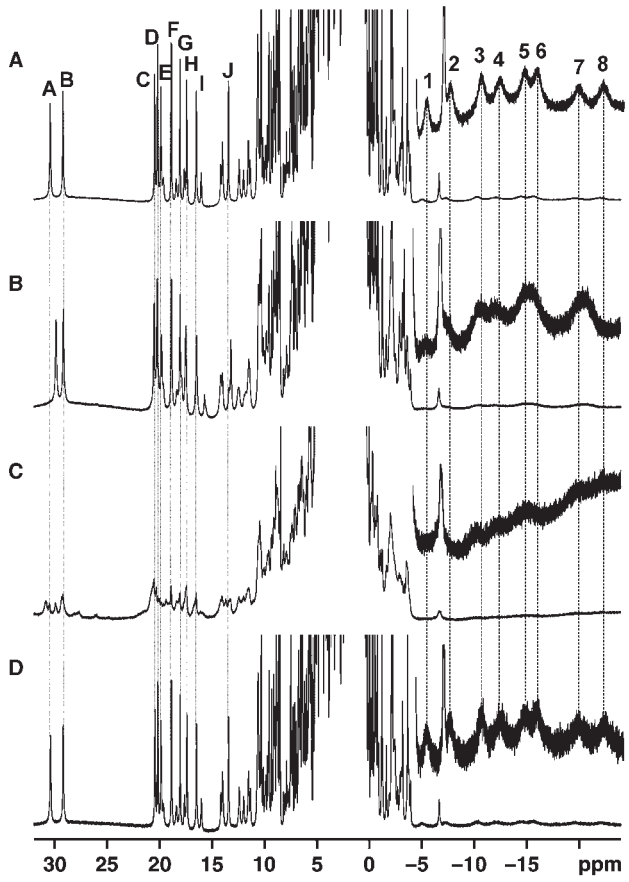

Fig. 2. **^{1}H NMR spectra of intact (A), misfolded B (B), misfolded A (C) and refolded (D) cytochromes c_3 at 500 MHz, p^{2}H 7.0 and 303 K. B, F and G, C and D, E and J, and A, H and I denote heme methyl signals belonging to hemes 1–4, respectively, and numbers 1–8 indicate C2 proton signals of the ligated histidines.**

The one-dimensional ^{1}H NMR spectra of the three forms are shown in Fig. 2. Although the macroscopic heme architecture of mfA and mfB cyts c_3 seemed to be similar to that of the intact form, judging from the CD spectra in Fig. 1, their microscopic heme environments, specified by coordination structures and interactions between hemes and surrounding amino acid residues, were quite different. Most heme methyl signals of the fully oxidized cyt c_3 appear in the region of 32–10 ppm due to paramagnetic effects (BioMagResBank entry 6572). Although the heme methyl signals of hemes 1 and 2 (signals B, F and G, and signals C and D, respectively, in Fig. 2) were identical to those of the intact form, those of hemes 3 and 4 (signals E and J, and signals A, H and I, respectively, in Fig. 2) were perturbed for mfB cyt c_3. On the other hand, all the heme methyl signals were perturbed and split into multiple ones in mfA cyt c_3. The C2 proton signals of ligated His appear in the region of –5 to –25 ppm (*22*). For mfB cyt c_3, these signals are well characterized and similar to those of intact cyt c_3, although some of them were perturbed (Fig. 2B). This revealed that eight ligands are the same as those in intact cyt c_3. On the other hand, these signals were almost broaden out for mfA cyt c_3, although they are still observable (Fig. 2C). Since the heme architecture is stabilized by the fifth and sixth coordination, all ligands in mfA should be intact in spite of more unfolded polypeptide structure in view of its CD and NMR spectra.

The ^{1}H–^{15}N HSQC (heteronuclear single-quantum coherence) spectra of three kinds of cyt c_3 are shown in Fig. 3. Since the assignment for fully oxidized intact cyt c_3 has been reported [(*23*) and BioMagResBank entry 6572], comparison of the ^{1}H–^{15}N HSQC spectra of mfA and mfB cyts c_3 with that of the intact form would provide detailed information. The residues showing large chemical shift perturbation are mapped on the tertiary structure of intact cyt c_3 (PDB entry 1J0O) as shown in Fig. 4. The perturbed region in mfB cyt c_3 comprised Lue84–Cys100, including half of helix 3, loop 5 and helix 4 (Fig. 4B). This region is located in between hemes 3 and 4. On the other hand, a wider region was perturbed in mfA cyt c_3 (Fig. 4A). The perturbed regions in both misfolded cyts c_3 included α-helices. The reduction of the secondary structure content in both misfolded cyts c_3 (Fig. 1) would be due to partial unfolding of the α-helices. So, we can conclude that mfA and mfB cyts c_3 are intact in terms of chemical composition and heme architecture, but are partially unfolded. This strongly suggests that they are not decomposed components of the intact cyt c_3 produced in the purification process, but are immature proteins. To characterize the nature of the immaturation, unfolding and refolding of mfA and mfB cyts c_3 were carried out.

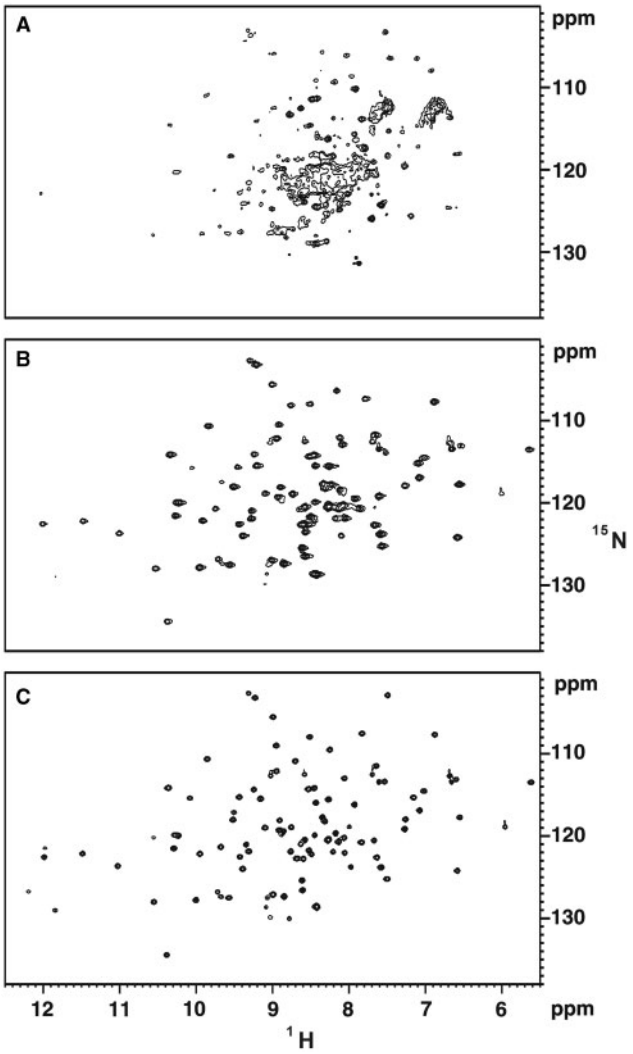

Fig. 3. **^{1}H–^{15}N HSQC spectra of (A) misfolded A, (B) misfolded B and (C) intact cytochromes c_3 at 600 MHz, p^{2}H 7.0 and 303 K.**

Urea and Gdn-HCl were used as denaturants for the unfolding and refolding of mfA and mfB cyts c_3. Unfolding and refolding were successfully carried out and gave the same results for both denaturants. At first, refolding of mfB cyt c_3 was performed because the perturbed region was small (Fig. 4). MfB cyt c_3 could be successfully refolded by means of the procedure described under 'Materials and Methods'. The yield of the intact cyt c_3 was calculated from the absorbance at 280, 409 and 552 nm, i.e. 87, 78 and 79%, respectively. The average yield of refolding was 81%. The refolded cyt c_3 was identical with the authentic form in terms of UV-visible spectrum, MALDI-TOF mass spectrum, N-terminal amino acid sequence (15 amino acids), ^{1}H spectrum (Fig. 2D) and ^{1}H–^{15}N HSQC spectrum (data, except for ^{1}H spectrum, not shown). MfA cyt c_3 could also be refolded by means of the same method. The average yield of refolding was 82%. Thus, the refolding yield was the same for mfA and mfB cyts c_3. This also supports the conclusion that all thioether linkages are intact.

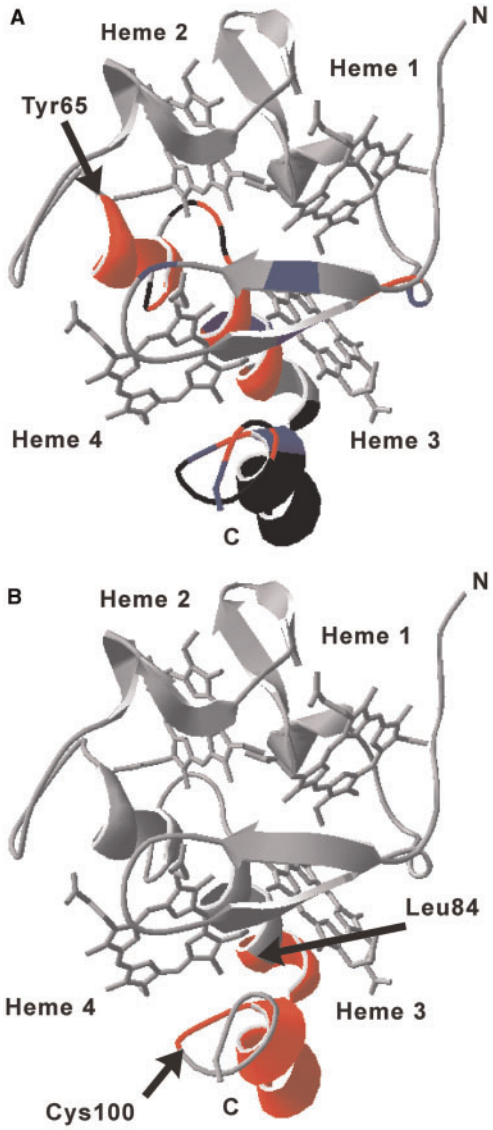

Fig. 4. **The residues showing large perturbations are mapped on the tertiary structure of intact cytochrome c_3 (PDB entry 1J0O). (A) Misfolded A and (B) misfolded B cytochromes c_3.** The perturbations are classified as $\{[(\Delta\delta_{HN})^2+(\Delta\delta_N/5)^2]/2\}^{1/2}<0.1$ (gray) and >0.1 (blue), and disappeared or greater shifted signals (red). Unidentified signals are coloured black. The figures were prepared with Swiss-PdbViewer (*28*).

DISCUSSION

A newly synthesized polypeptide usually folds into a functional structure through a multistep pathway, including a molten globule state. This is called on-pathway folding. A protein, however, often fails to fold correctly, which is called off-pathway folding. When a protein undergoes off-pathway folding, a molecular chaperone helps it return to on-pathway folding (*24*). If a protein continues off-pathway folding, it is degraded by proteases (*24*). In the case of *c*-type cytochromes, heme groups have to be covalently linked during the folding process. Apoproteins exhibiting failure as to the linking

of heme will be degraded immediately by specific proteases (*25*). Physiologically, this is called the maturation process. This has been extensively investigated for monoheme cyt *c* [reviewed in (*1*)]. For the first time, this work has shed light on the process of maturation of tetraheme cyt c_3.

Two kinds of misfolded proteins, mfA and mfB cyts c_3, were obtained in a *Shewanella* expression system. The ratio of mfA, mfB and intact cyts c_3 expressed in *Shewanella* at various temperatures was constant, i.e. roughly 2:2:9, respectively. This means that about one-third of newly synthesized cyt c_3 undergoes off-pathway folding in spite of the presence of Ccm proteins. From the characterization performed in this work, it can be concluded that both mfA and mfB cyts c_3 have an intact polypeptide, the correct thioether linkage between the peptide and four hemes, and an almost mature heme architecture with the correct ligands at the fifth and sixth coordination sites. They only differ in the extent of peptide folding. Also, incorrectly folded regions are mainly helices in the C-terminal region. In the case of mfA cyt c_3, chemical shift perturbation was observed from Tyr65 all the way to the C-terminus (Fig. 3A). The aromatic ring of Tyr65 is involved in the formation of the hydrophobic core together with four hemes (*20*). This is also the starting residue of helix 2. In the case of mfB cyt c_3, on the other hand, perturbation was observed in the region of Lue84–Cys100, which includes a part of helix 3 and the whole of helix 4. The region includes Cys82 (the heme 3 attachment site), His83 (the fifth ligand of heme 3) and Cys100 (the heme 4 attachment site).

Since the sixth coordination should play an important role in the formation of the heme architecture, they should be coupled with each other. This seems to take place automatically. The heme architecture also forms the hydrophobic core of the protein. Helices 2 and 3 are involved in the formation of the hydrophobic core, in contrast to the other parts of the polypeptide. Therefore, the formation of the heme architecture should also be coupled with the helix formation in this region. However, there are two coordination sites (His70 and His83 as the sixth and fifth ligands of hemes 4 and 3, respectively) and two thioether linkages (Cys79 and Cys82 for heme 3, and Cys100 and Cys105 for heme 4) in this short stretch. This would suppress the rate of trial-and-error for the helix formation in this region, resulting in off-pathway folding of mfA cyt c_3. Since this region is located inside the protein, such misfolding will also affect the microenvironments of heme groups, as observed in Fig. 2C. In the case of mfB cyt c_3, helices 3 and 4 are fixed to the tetraheme architecture through two heme attachment sites. Once it misfolds, restoration of the correct helix conformation is not easy because of the two fixed ends (Cys82 and Cys100), resulting in another off-pathway folding. The occurrence of two types of off-pathway folding suggests that they are the consequence of the tetraheme architecture formation coupled with the coordination of the sixth ligands. In the Ccm system of *Shewanella*, the helix formation is not well coupled with the tetraheme architecture.

Usually, proteins undergoing off-pathway folding are helped by chaperone proteins to return to on-pathway folding. Since about 80% of mfA and mfB cyts c_3 were refolded into the intact cyt c_3 with denaturants, a chaperone could also be involved in this case. Although *S. oneidensis* synthesizes *c*-type tetraheme proteins such as small tetraheme cytochrome *c* (*26*) and flavocytochrome *c* (*27*), hemes line up linearly in the proteins (PDB entries 1M1P and 1D4C, respectively). Since cyt c_3 has a cyclic heme architecture, the configuration should be much more complicated than a linear one. This would be the reason why the *c*-type heme protein maturation system used in *S. oneidensis* is insufficient for the maturation of cyt c_3. Actually, no misfolded proteins were found in SRB. The maturation system in SRB should have a chaperone-like function to help the sixth ligand coordination, the formation of the heme architecture, and the helix formation take place cooperatively, leading to on-pathway folding. However, it is not clear if the Ccm system of *S. oneidensis* has a chaperone-like function for a linear tetraheme cytochrome *c*. The overexpression of a *c*-type multiheme protein is quite difficult. The *Shewanella* expression system is simple and useful in spite of the problems indicated in this work. Actually, the refolding procedure developed in this work has increased the amount of cyt c_3 produced by roughly 1.4 times compared with that previously reported (*17*).

We thank Dr Kei-ichi Yamaguchi (Osaka University) for the help in the CD experiments and to Prof. Takahisa Ikegami (Osaka University) for the help in the NMR measurements. This research was partly supported by a Grant-in-Aid for Scientific Research on Priority Areas from the Ministry of Education, Science, Technology, Sport and Culture of Japan.

REFERENCES

1. Cianciotto, N.P., Cornelis, P., and Baysse, C. (2005) Impact of the bacterial type I cytochrome *c* maturation system on different biological processes. *Mol. Microbiol* **56**, 1408–1415
2. Allen, J.W.A., Leach, N., and Ferguson, S.J. (2005) The histidine of the *c*-type CXXCH haem-binding motif is essential for haem attachment by the *Eschirichia coli* cytochrome *c* maturation (Ccm) apparatus. *Biochem. J.* **389**, 587–592
3. Winkler, J.R. (2004) Cytochrome *c* folding dynamics. *Curr. Opin. Chem. Biol.* **8**, 169–174
4. Ambler, R.P. (1980) In: *From Cyclotrons to Cytochromes* (Robinson, A.B. and Kaplan, K.O., eds) pp. 263–279 Academic Press, London
5. Higuchi, Y., Kusunoki, M., Matsuura, Y. *et al.* (1984) Refined structure of cytochrome c_3 at 1.8 Å resolution. *J. Mol. Biol.* **172**, 109–139
6. Ozawa, K., Takayama, Y., Yasukawa, F. *et al.* (2003) Role of the aromatic ring of Tyr43 in tetraheme cytochrome c_3 from *Desulfovibrio vulgaris* Miyazaki F. *Biophys. J.* **85**, 3367–3374
7. Harada, E., Fukuoka, Y., Ohmura, T. *et al.* (2002) Redox-coupled conformational alterations in cytochrome c_3 from *D. vulgaris*. Miyazaki F on the basis of its reduced solution structure. *J. Mol. Biol.* **319**, 767–778
8. Pollock, W.B.R., Chemerika, P.J., Forrest, M.E. *et al.* (1989) Expression of the gene encoding cytochrome c_3 from *Desulfovibrio vulgaris* (Hildenborough) in *Escherichia coli*: export and processing of the apoprotein. *J. General Microbiol.* **135**, 2319–2328

9. Kitamura, M., Ozawa, K., Kojima, S. *et al.* (1993) The primary structure of pre-cytochrome c_3 from *Desulfovibrio vulgaris* (Miyazaki F) as determined by nucleotide sequencing of its gene and partial amino acid sequencing. *Protein Seq. Data Anal.* **5**, 193–196
10. Cannac, V., Caffrey, M.S., Voordouw, G. *et al.* (1991) Expression of the gene encoding cytochrome c_3 from the sulfate-reducing bacterium *Desulfovibrio vulgaris* in the purple photosynthetic bacterium *Rhodobacter sphaeroides*. *Arch. Biochem. Biophys.* **286**, 629–632
11. Costa, P.N., Conte, C., and Saraiva, L.M. (2000) Expression of a *Desulfovibrio* tetraheme cytochrome *c* in *Eschericia coli*. *Biochem. Biophys. Res. Commun.* **268**, 688–691
12. Herbaud, M.-L., Aubert, C., Durand, M.-C. *et al.* (2000) *Escherichia coli* is able to produce heterologous tetraheme cytochrome c_3 when the ccm genes are co-expressed. *Biochim. Biophys. Acta* **1481**, 18–24
13. Arslan, E., Schulz, H., Zufferey, R. *et al.* (1998) Overproduction of the *Bradyrhizobium japonicum* *c*-type cytochrome subunits of the cbb_3 oxidase in *Escherichia coli*. *Biochem. Biophys. Res. Commun.* **251**, 744–747
14. Ozawa, K., Tsapin, A.I., Nealson, K.H. *et al.* (2000) Expression of a tetraheme protein, *Desulfovibrio vulgaris* Miyazaki F cytochrome c_3, in *Shewanella oneidensis* MR-1. *Appl. Environ. Microbiol.* **66**, 4168–4171
15. Kranz, R., Lill, R., Goldman, B. *et al.* (1998) Molecular mechanisms of cytochrome *c* biogenesis: three distinct systems. *Mol. Microbiol.* **29**, 383–396
16. Cianciotto, N. P., Cornelis, P., and Baysse, C. (2005) Impact of the bacterial type I cytochrome *c* maturation system on different biological processes. *Mol. Microbiol.* **56**, 1408–1415
17. Ozawa, K., Yasukawa, F., Fujiwara, Y. *et al.* (2001) A simple, rapid, highly efficient gene expression system for multiheme cytochrome *c*. *Biosci., Biotechnol., Biochem.* **65**, 185–189
18. Feng, Y., Sligar, S.G., and Wand, A. J. (1994) Solution structure of apocytochrome b_{562}. *Nat. Struct. Biol.* **1**, 30–35
19. Ozawa, K., Takayama, Y., Yasukawa, F. *et al.* (2003) Role of the aromatic ring of Tyr43 in tetraheme cytochrome c_3 from *Desulfovibrio vulgaris* Miyazaki F. *Biophys. J.* **85**, 3367–3374
20. Takayama, Y., Harada, E., Kobayashi, R. *et al.* (2004) Roles of non-coordinated aromatic residues in redox regulation of cytochrome c_3 from *Desulfovibrio vulgaris* Miyazaki F. *Biochemistry* **43**, 10859–10866
21. Takayama, Y., Kobayashi, Y., Yahata, N. *et al.* (2006) Specific binding of CO to tetraheme cytochrome c_3. *Biochemistry* **45**, 3163–3169
22. Yahata, N., Ozawa, K., Tominoto, Y. *et al.* (2006) Roles of charged residues in pH-dependent redox properties of cytochrome c_3 from *Desulfovibrio vulgaris* Miyazaki F. *Biophysics* **2**, 45–56
23. Yahata, N., Saitoh, T., Takayama, Y. *et al.* (2006) Redox interaction of cytochrome c_3 with [NiFe] hydrogenase from *Desulfovibrio vulagaris* Miyazaki F. *Biochemistry* **45**, 1653–1662
24. Alberts, B., Johnson, A., Lewis, J. *et al.* (2001) *Molecular Biology of the Cell*. 4th edn. pp. 355–357 Garland Science, Tailor & Francis Group
25. Thöny-Meyer, L., Künzler, P., and Hennecke, H. (1996) Requirements for maturation of *Bradyrhizobium japonicum* cytochrome c_{550} in *Escherichia coli*. *Eur. J. Biochem.* **235**, 754–761
26. Leys, D., Meyer, T.E., Tsapin, A.S. *et al.* (2002) Crystal structures at atomic resolution reveal the novel concept of "electron-harvesting" as a role for the small tetraheme cytochrome *c*. *J. Biol. Chem.* **277**, 35703–35711
27. Leys, D., Tsapin, A.I., Nealson, K.H. *et al.* (1999) Structure and mechanism of the flavocytochrome *c* fumarate reducease of *Shewanella putrefaciens* MR-1. *Nat. Struct. Biol.* **6**, 1113–1117
28. Guex, N. and Peitsch, M.C. (1996) Swiss-PDBViewer: a fast and easy-to-use PDB viewer for Macintosh and PC. *Protein Data Bank Quarterly Newsletter* **77**, 7